

Fermilab Proposal No. 788  
Scientific Spokesperson:  
R. H. Bernstein  
Fermilab MS 122  
(312)840-2035  
BITNET RHBOB@FNAL

A Proposal  
for a Neutrino Oscillation Experiment  
in a Tagged Neutrino Line

R.H. Bernstein, F. Borcharding, D. Jovanovic, M.J. Lamm  
Fermilab

F. Vannucci  
LPHNE, University of Paris VI and VII

September, 1988

## ABSTRACT

We propose a study of neutrino oscillations and cross-sections in a tagged neutrino line. A  $K_L$  beam and the decay modes  $K_L \rightarrow \pi e \nu_e$  and  $K_L \rightarrow \pi \mu \nu_\mu$  will provide the neutrino flux. An upstream tagging spectrometer will identify the hadron and lepton and reconstruct the  $K_L$  decay; the lepton identification will specify the neutrino as  $\nu_e$  or  $\nu_\mu$  and distinguish neutrinos from antineutrinos at the decay vertex. Downstream, the CCFR neutrino detector will be used to associate the  $K_L$  decay with a neutrino interaction, measure the neutrino energy and analyze outgoing muons. Monte-Carlo studies predict that 30K  $\nu_e$  and 20K  $\nu_\mu$  interactions can be obtained in two fixed target runs at the Tevatron. The experiment will significantly improve existing oscillation measurements. It will test the channel  $\nu_e \rightarrow \nu_\mu$  down to  $\sin^2 2\theta_{e\mu} > 3 \times 10^{-4}$ , an order of magnitude smaller than current determinations. We can also study the oscillation mode  $\nu_e \rightarrow \nu_\tau$  with a sensitivity of  $\sin^2 2\theta_{e\tau} > 2 \times 10^{-3}$  for  $\Delta m_{e\tau}^2 > 100$  ( $eV/c^2$ )<sup>2</sup>. The expected sensitivity in the  $\nu_e \rightarrow \nu_\tau$  oscillation channel represents roughly a factor of seventy improvement in mixing angle over previous efforts. This sample will also determine the charged and neutral current cross-sections for  $\nu_\mu$  and the total cross-section for  $\nu_e$ , all to 1-2%, in the energy range of 30-400 GeV. The experiment would provide a unique and precise measurement of the  $\nu_e$  cross-section at high energy and would improve the existing  $\nu_\mu$  cross-section measurements by a factor of three. Finally, the significant  $K_L$  flux (more than  $10^{14}$  decays in the experiment) provides a opportunity for rare  $K_L$  decay searches as well.

## Table of Contents

1. Motivation and Method
    - (a) Oscillation Phenomenology
    - (b) Previous Experiments and Results
    - (c) Neutrino Tagging
    - (d) Physics Goals of the Tagged Line
  2. Apparatus
    - (a) Target and Beam Line
    - (b) Tagging Spectrometer
    - (c) Neutrino Detector
  3. Rates and Acceptances
  4. Triggering
  5. Backgrounds and Systematic Errors
  6. Schedule
  7. Long-Term  $K_L$  Studies
  8. Conclusions
-

## List of Figures

- Fig. 1. Existing Limits in the Oscillation Channels  $\nu_\mu \rightarrow \nu_e$ ,  $\nu_e \rightarrow \nu_\tau$ , and  $\nu_\mu \rightarrow \nu_\tau$
- Fig. 2. A Schematic of a Neutrino Tagger
- Fig. 3. Limits in the  $\nu_e \rightarrow \nu_\mu$  search
- Fig. 4. Limits in the  $\nu_e \rightarrow \nu_\tau$  search
- Fig. 5. Opposite-Sign Dimuon Production
- Fig. 6.  $\sigma_\nu$  vs.  $E_\nu$  Compared to Previous World Data
- Fig. 7. The slope  $\alpha = \sigma_\nu/E_\nu$  Compared to Previous World Data
- Fig. 8. A Schematic of a Beam Line for the Proposed Experiment
- Fig. 9. A Schematic of the Lab E Neutrino Detector
- Fig. 10. A Comparison of the Observed  $K_L$  Spectrum to the Predicted Spectrum  
from the Flux Program
- Fig. 11. A Flux Map for Neutrons
- Fig. 12. A Flux Map for  $\Lambda^0$
- Fig. 13. A Flux Map for Produced  $K_L$
- Fig. 14. A Flux Map for Decaying  $K_L$
- Fig. 15. The  $\nu$  Spectrum Incident on the Detector
- Fig. 16. A Schematic of a Mistag
- Fig. 17. The Difference in the Reconstructed and True x-coordinate of the Decay Vertex
- Fig. 18. The Difference in the Reconstructed and True z-coordinate of the Decay Vertex
- Fig. 19. The Difference over the Sum of the Two Solutions for the  $K_L$  Energy
- Fig. 20. The Distance from the Reconstructed to True Impact Point in the  
 $\nu$  Detector

Fig. 21. The Difference of the Predicted and Measured  $\nu$  Energy, Divided by the Predicted Value

Fig. 22. The Source of "Same-Sign" Dimuons

Fig. 23. The  $p_T$  of the Muon with Respect to the Hadronic Shower

## I. Motivation and Method

The discovery of neutrino oscillations, in which a neutrino of one species oscillates into a neutrino of a different species (for example,  $\nu_e \rightarrow \nu_\mu$ ), would force a profound change in our understanding of nature. It would violate the conservation of lepton number, which would have a significant impact on grand unification theories and it would imply that neutrinos are massive, which has cosmological implications; furthermore, it would open a wide number of new questions concerning the sources of neutrino masses and mixing angles and their relationships to the quark and lepton sectors. The study of these topics could recreate our picture of the “standard model” and provide a new set of questions and experiments for many years to come. The phenomenon of neutrino oscillations is thus worthy of continuing experimental effort whenever the possibility of a significantly improved measurement exists.

### A. Oscillation Phenomenology<sup>1</sup>

Neutrino oscillations are transitions among different neutrino species. (In this discussion we limit ourselves to a two-component system for simplicity, although oscillations among all species are allowed.) Neutrino oscillations are similar to  $K^0/\bar{K}^0$  oscillations<sup>2</sup>; the weak interaction which does not conserve strangeness in the neutral kaon system would be analogous to some new interaction in the neutrino system which does not conserve individual lepton numbers:  $\nu_e$  and  $\nu_\mu$  are analogous to  $K^0$  and  $\bar{K}^0$  and the mass eigenstates are now  $\nu_1$  and  $\nu_2$  instead of  $K_1$  and  $K_2$ . New mixing angles are required which are analogous to the Kobayashi-Maskawa angles in the quark matrix. In a two-component system one finds, for a  $\nu$  traveling a distance  $R(\text{km})$ :

---

<sup>1</sup>A recent review is Bilenky and Petcov, Massive Neutrinos and Neutrino Oscillations, RMP 59, No 3 (1987) 671-754.

<sup>2</sup>The differences arise because the  $\nu$  is a fermion and the  $K^0$  is a boson.

$$P(\nu_1 \rightarrow \nu_2) = \sin^2 2\theta_{12} \sin^2 \pi R/L$$

where

$$L = 2.5 E_\nu / \Delta m^2 \quad km^* GeV / (eV)^2$$

and

$$\Delta m^2 = m_1^2 - m_2^2$$

where  $m_1$  and  $m_2$  are the masses of the mass eigenstates  $\nu_1$  and  $\nu_2$ . There are then two requirements for mixing:

- (1) the mixing angle  $\theta_{12}$  must be non-zero;
- (2) at least one neutrino species must be massive.

## B. Previous Experiments and Results

A straightforward way to look for oscillations is to place two neutrino detectors at two different distances from a target and look for a change in rate of any given neutrino species: if neutrinos oscillate, the rates will change as the neutrinos propagate. This method has several advantages: (1) it checks oscillations from a given channel into all possible channels simultaneously, and (2) it does not depend on detailed knowledge of the production rates of the various neutrino species at the target. However, it has a significant disadvantage: since one must compare the rates among different detectors, the statistical power is that of the ratio among the detectors, and hence only grows as  $\sqrt{N}$  where  $N$  is the number of neutrino events. This technique is generally known as a disappearance method: the first detector “measures” the flux and the second checks for a disappearance of that species, signalling an oscillation.

A second method is based on the "appearance" of a new species. In this method a single detector is used. Here the spectrum of neutrinos from the production target is used to predict the rate at the neutrino detector. The analysis is then based on searching for a discrepancy from the predicted rate and the statistical power grows with  $N$ . Since most neutrino beams are predominantly  $\nu_\mu$  (they arise from charged beams and the  $K\pi_2$  mode) experiments have typically searched for  $\nu_\mu \rightarrow \nu_e$  oscillations. This method then has two disadvantages. First, any systematic error in the initial spectrum will signal an oscillation:  $\nu_e$  contaminations in standard  $\nu_\mu$  beams are typically 1% and when searching for new physics, one must know this 1% very precisely. Second, a  $\nu_e$  signal has several significant backgrounds. A  $\nu_\mu$  neutral current interaction may produce  $\pi^0$ 's, which will then decay; the resultant photons may then shower, resulting in electron tracks which can fake a  $\nu_e$  charged current signal. This background is subtracted by demanding the track point back to the  $\nu$  vertex, requiring excellent tracking and highly efficient chambers. The  $\nu_e$  beam contamination and the  $\pi^0$  background have limited the regions probed in accelerator experiments to about  $P(\nu_\mu \rightarrow \nu_e) = (0.5 - 1.0)\%$ . In order to make significant improvements, new techniques will be required.

The present best limits for the channels  $\nu_\mu \rightarrow \nu_e$ ,  $\nu_e \rightarrow \nu_\tau$ , and  $\nu_\mu \rightarrow \nu_\tau$  are shown in Fig. 1, including both reactor and accelerator searches.<sup>3</sup> There is no compelling evidence of oscillations in the regions that have been searched.

---

<sup>3</sup>We have used data reviewed in W.Y. Lee, Neutrino '86 (proceedings), World Scientific Publishing Co., 1986, p.157, and in F. Vannucci, BNL Neutrino Workshop (Proceedings), BNL52079 UC-34-D, from which we have adapted the Figure.



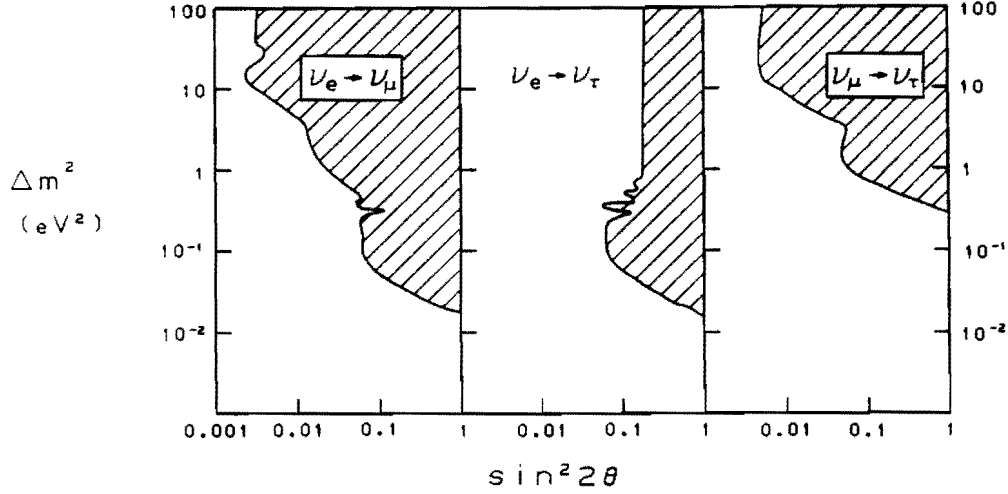


Fig. 1. Existing Limits in the oscillation channels  $\nu_\mu \rightarrow \nu_e$ ,  $\nu_e \rightarrow \nu_\tau$ , and  $\nu_\mu \rightarrow \nu_\tau$ .

### C. Neutrino Tagging

A third method exists which is free of the above problems, allowing us to probe probabilities of oscillation down to 0.01% instead of 1%. In it, a spectrometer tags, on an event-by-event basis, the neutrino species at the production vertex. Then a neutrino detector checks that the neutrino interaction is of the correct type. There are no errors from simulations of the beam content since the species of every neutrino is determined at the point of production. The sensitivity of this method improves as  $1/N$  since no ratios between detectors are formed. A schematic tagger is shown in Fig. 2; the upstream detector determines the momenta and charges of the pion and lepton and identifies the lepton as an electron or a muon. The downstream detector records the neutrino interaction, measuring its energy and the momentum and charge of outgoing muons. The charge of the lepton in the tagger must

have the opposite charge of the muon in the neutrino detector (unless a  $\nu_\mu \rightarrow \bar{\nu}_\mu$  oscillation has occurred). This “charge-matching” is a powerful tool of the tagging technique and we will use it frequently.

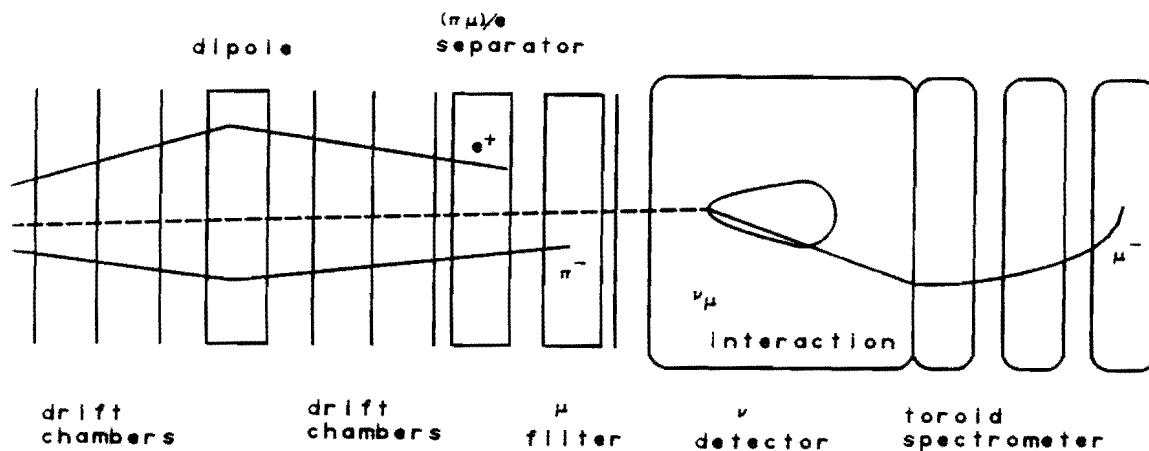


Fig. 2. A schematic of a neutrino tagger. The beam direction is from the left; a  $Ke_3$  decay is pictured in the tagger, with the  $\pi$  and  $e$  identified and momentum analyzed. The neutrino detector downstream detected a  $\nu_\mu$  charged-current interaction, signaling an oscillation  $\nu_e \rightarrow \nu_\mu$ .

In a  $\nu_\mu \rightarrow \nu_e$  search, the backgrounds from  $\nu_\mu$  neutral current events persist. If one turns the search around, and studies  $\nu_e \rightarrow \nu_\mu$  instead, the signal becomes the presence of an energetic muon instead of its absence. This cannot be done in standard  $\nu$  beams because they are predominantly (99%)  $\nu_\mu$ ; however, a neutral beam containing  $K_L$  will provide a neutrino source with 60%  $\nu_e$ .<sup>4</sup> One significant background in the  $\nu_\mu$  search is the production of muons from  $\pi/K$  decay in the hadronic shower. This rate has been carefully studied by like-sign dimuon experiments and occurs at a rate of  $10^{-4}$  of all charged current events. We

<sup>4</sup>The branching fractions for  $K_L$  decay are  $\text{BR}(K_L \rightarrow \pi e \nu_e) = 38.7\%$ ,  $\text{BR}(K_L \rightarrow \pi \mu \nu_\mu) = 27.1\%$  (from the Particle Data Book).

set the level with the data from E744/E770 and simulate the kinematics with the E744/E770 Monte Carlo. We predict there will be approximately 5.4 events in the 30K sample from this source of background before we apply cuts.

A second background in the tagging method arises from mistags. Let us imagine that a  $K\mu_3$  decay occurs close in time to a  $Ke_3$  decay, and the tagger accepts the  $(\pi e)$  products but the  $(\pi\mu)$  pair escapes; then if the  $\nu_\mu$  interacts in the neutrino detector, the combination  $(\pi e)_{\text{tagger}}$  and  $\nu_\mu$  will appear to be an oscillation. We reject this background by reconstructing the neutral kaon from the tagger and then predicting the impact point, energy, and species of the neutrino. The predicted values may then be compared those measured for the detected neutrino to reject spurious coincidences. An additional order-of-magnitude rejection comes from demanding the  $(\pi e)$  and the  $\nu$ -interaction occur within the same RF bucket. After applying appropriate cuts, we approximately halve the sample to 16K and reduce the background to 0.3 events. The rejection of this background will be covered more fully in Section V.

#### D. Physics Goals of the Tagged Line

A simulation of the experiment has indicated that a tagging experiment at FNAL could explore new regions of mixing angle. Fig. 3 compares the exclusion curve for the  $\nu_e \rightarrow \nu_\mu$  channel from BNL734 to the power of the proposed tagging experiment at FNAL with 16K  $\nu_e$  tags. The 16K sample probes a factor of ten lower in mixing angle (but does not add to the small  $\Delta m^2$  region). If we were to observe a signal, one could also check particle/antiparticle rates (the tagger determines the charge of the lepton) opening the possibility of CP-nonconservation studies in the neutrino sector.

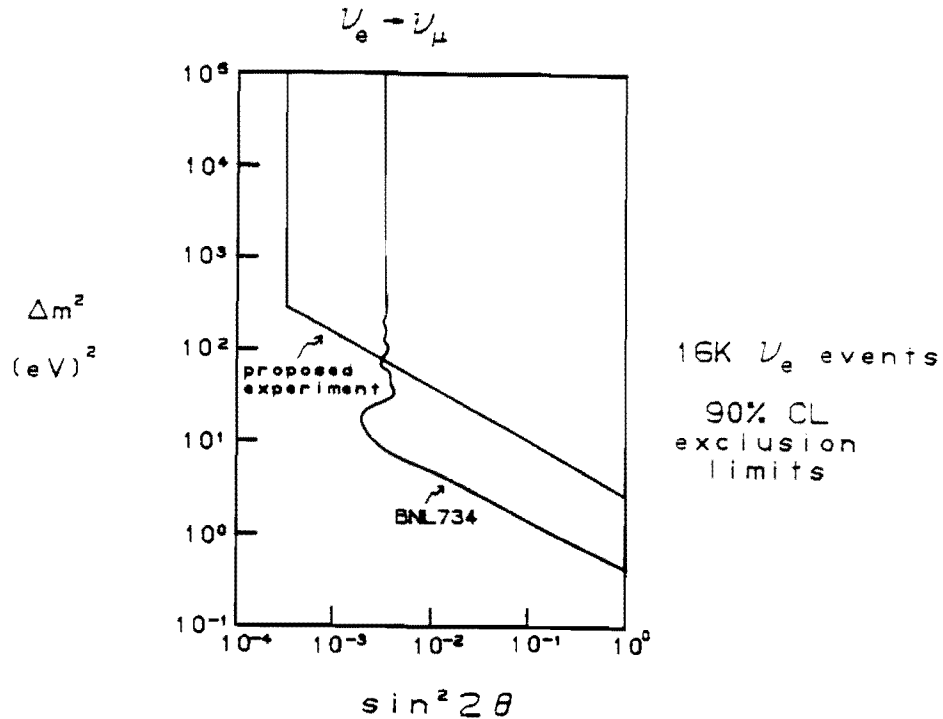


Fig. 3. Limits achievable in the proposed experiment compared to BNL734. The proposed experiment reaches a factor of 20 lower in  $\sin^2 2\theta$  but does not probe lower in  $\Delta m^2$ .

The oscillation channel  $\nu_e \rightarrow \nu_\tau$  has a poor limit in  $\sin^2 2\theta$ , only 0.12 for large  $\Delta m^2$ . Here, we would use the reaction  $\nu_\tau N \rightarrow \tau X$ ,  $\tau \rightarrow \mu \nu \nu$  and observe the  $\mu$  in the neutrino detector. The branching fraction  $\tau \rightarrow \mu \nu \nu$  is 17%, decreasing the statistical power relative to a  $\nu_e \rightarrow \nu_\mu$  search (so the 16K  $\nu_e \rightarrow \nu_\mu$  sample has the statistical power of 2700 events for the  $\nu_e \rightarrow \nu_\tau$  search). We have no way of distinguishing muons from  $\nu_\mu$  charged-current events from muons from  $\tau$  decay. However, the region to which we are sensitive has already been excluded in  $\nu_\mu \rightarrow \nu_e$  searches, so we would know the oscillation would be  $\nu_e \rightarrow \nu_\tau$  and

not  $\nu_e \rightarrow \nu_\mu$ .<sup>5</sup> Fig. 4 shows the expected power of this experiment (statistical error only) compared to previous measurements: we see approximately a factor of 70 improvement over previous limits in  $\sin^2 2\theta_{e\tau}$ , from  $\sin^2 2\theta_{e\tau} < 0.1$  to  $\sin^2 2\theta_{e\tau} < 0.0016$  (@ 90%CL). We expect there to be approximately 0.3 events of background from mistags and an approximately equal number from “same-sign” sources in this 16K sample. A search at small mixing angle and large  $\Delta m^2$  is certainly of great interest. Furthermore, astrophysical arguments constrain  $m_{\nu_\tau} < 65 \text{ eV}/c^2$ ; this mass range makes  $\nu_\tau$  a popular dark-matter candidate.<sup>6</sup> Our search would be sensitive down to  $m_{\nu_\tau} \geq 10 \text{ eV}/c^2$  for  $\theta_{e\tau} > .017$ , certainly an important region to cover.

---

<sup>5</sup>Unless there is a fortuitous CP-violation in the  $\nu$  mixing matrix, in which case  $\nu_e \rightarrow \nu_\mu$  is not necessarily the same as  $\nu_\mu \rightarrow \nu_e$ .

<sup>6</sup>See Neutrino Masses and Neutrino Astrophysics (Telemark IV), 1987 (World Scientific Press) for a variety of papers on these topics.

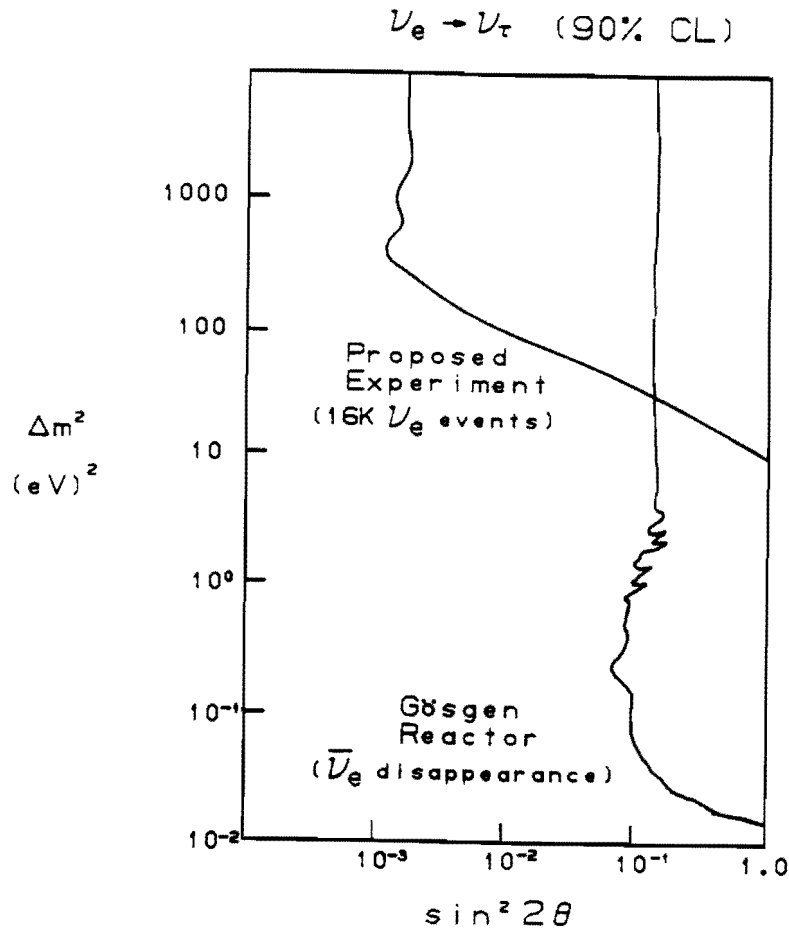


Fig. 4. The proposed limit for  $\nu_e \rightarrow \nu_\tau$  compared to the best previous experiment, a  $\bar{\nu}_e$  total disappearance experiment in a reactor. If we assume  $m_{\nu_e} = 0$ ,  $\Delta m^2 = m_{\nu_\tau}^2$  and hence the experiment probes down to  $m_{\nu_\tau} \geq 10$  eV for small mixing angles.

Neutrino/antineutrino oscillations (for  $\nu_\mu$  only, where we can determine the lepton charge) could also be studied in the tagged line. The limitation of previous experiments was knowledge of the beam composition; in the tagged line this uncertainty would vanish and the only background would be muoproduction in the shower. We would search for the production

of a positive muon in the neutrino detector along with a negative muon in the tagger. The dominant background would arise from charm production, through the process shown in Fig. 5. This process, the source of “opposite-sign” dimuons, has been accurately measured and modeled in the CCFR apparatus;<sup>7</sup> we use the CCFR Monte Carlo and the measured rates to simulate the background. The background is suppressed in two ways: first by comparing the charge of the muon in the tagger to the charge of the muon in the neutrino detector: an oscillation would result in the muons having opposite charge, while a muon from charm decay would have the same charge as the tagger muon. Second, the muon produced from charm decay generally has a lower energy than the current muon and would have to be detected, while the current muon would have to range out in the hadronic shower and escape detection. A second source is from neutral current  $\nu_\mu$  interactions where the  $\mu$  from charm decay is accepted. The outgoing  $\nu_\mu$  will escape with large missing energy and we may demand the predicted energy from the tagger matches the measured energy in the neutrino detector. These requirements lower the background from charm production to less than an event and we could set limits on  $\nu_\mu \rightarrow \bar{\nu}_\mu$  oscillations to  $10^{-4}$  at 90%CL. This represents a factor of two improvement over previous measurements (the best of which actually saw a  $2\sigma$  effect and interpreted it as a 90%CL).<sup>8</sup> There are a variety of precision cross-section measurements which could be performed in the tagged line. Determinations of the muon neutrino cross-section have been limited by uncertainties in the initial flux to roughly the 3-5% level.<sup>9</sup> In the tagged line for as few as 1000 events, about two weeks at the proposed flux, this limit would be exceeded! A sample of tagged data could be used to predict the number of neutrinos that would strike the neutrino detector; we would then compare the ob-

<sup>7</sup>Lang et al., Z. Phys. C33(1987),483; preliminary results from the E744 run are found in Foudas et al., presented at 3rd Lake Louise Winter Institute, Fermilab Preprint 79,339.

<sup>8</sup>S.R. Mishra, “A Study of Wrong Sign Muon and Trimuon Events in Neutrino-Nucleon Scattering”, PhD Thesis, Columbia University (1986) Nevis Preprint #259.

<sup>9</sup>Fisk and Sciulli, “Charged Current Neutrino Interactions”, Ann. Rev. Nucl. Sci. 32 (1982), 499.

served to predicted number to determine the cross-section. A small systematic error would arise from the quality of the prediction: the acceptance of neutrino events in the CCFR neutrino detector is about 80% for the expected charged current events, and the general good agreement of the CCFR Monte Carlo with the data lead us to believe the error on the acceptance is no worse than 5% of itself, leading to a 1% systematic error. There are small systematic errors from misidentification of leptons in the tagger, leading to a rejection of the event: the rejection is no larger than  $10^{-4}$  of all neutrino interactions, as will be shown later.

The energy-dependence of the cross-section could be studied as well. Fig. 6 shows  $\sigma_\nu/E_\nu$  for this experiment compared to the previous world sample.<sup>10</sup> First, we see the range of useful measurement is extended from 250 GeV to 400 GeV; second, the systematic errors will be smaller because the tagged line has no uncertainties from flux monitoring devices. Cerenkov counters were used to determine the relative  $\pi/K$  content in E616/701 at Fermilab, together with ion chambers to measure the absolute flux during the fast spill. Each of these devices contributed systematic errors to the cross-section determination and neither would be required in the tagged line.<sup>11</sup> Fig. 7 shows the determination of the slope in this experiment plotted along with existing results; the slope, which is directly proportional to the integral of  $F_2$  (for neutrinos, and  $F_3$  for antineutrinos), is determined to approximately 1%.<sup>12</sup> (We have not included the propagator effects on the cross-section; they will be 4-5% and we should be able to see them at the 2-3  $\sigma$  level).

---

<sup>10</sup>Particle Data Book, p. 153.

<sup>11</sup>R. Blair et al., NIM 228:281,1984.

<sup>12</sup>The E744/E770 data sample may be able to determine the  $\sigma_{\nu_e}$  slope to similar accuracy; however, it cannot set an absolute level except by Monte Carlo.



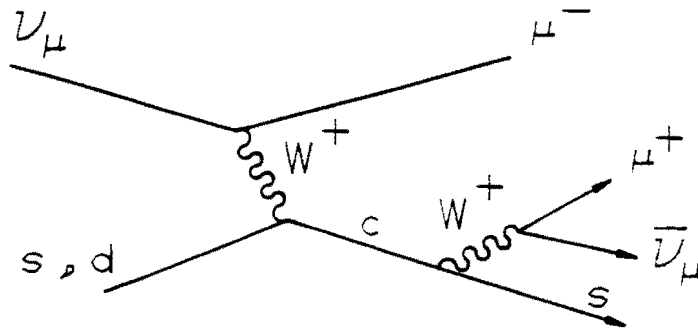


Fig. 5. The process for opposite sign dimuon production; an  $s$  or  $d$  quark absorbs a  $W$ , turning into a charmed quark, which then decays.

The  $\nu_e$  total cross-section will be determined to similar accuracy; we measure only the  $\nu_e$  total cross-section because we cannot track an electron in the CCFR detector and therefore cannot separate charged current from neutral current  $\nu_e$  interactions. The CHARM collaboration has measured  $\sigma(\nu_e)/\sigma(\nu_\mu) = 1.20 \pm 0.11$  for charged current events.<sup>13</sup> Hence a 1% measurement would reduce the errors by an order-of-magnitude and provide a precise test of universality.

<sup>13</sup>J.V. Allaby et al., Phys. Lett. B179(1986), 301.

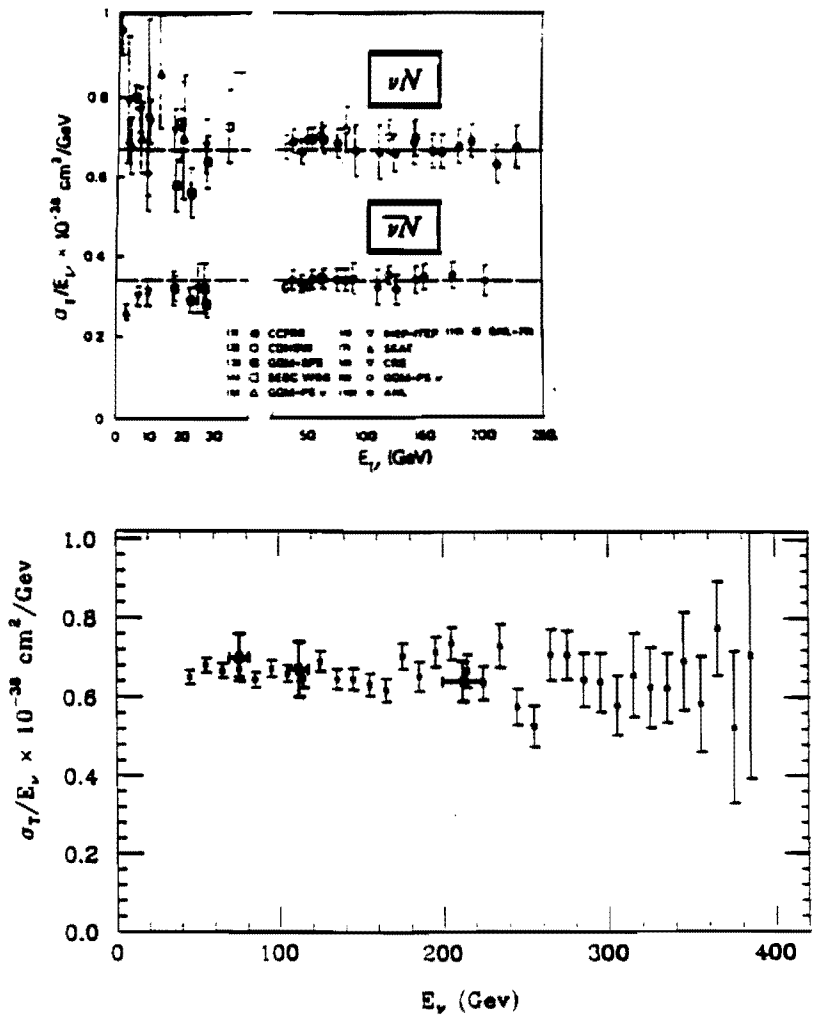


Fig. 6. A comparison of  $\sigma_\nu/E_\nu$  in this experiment to previous world data. The top plot is the compilation from the Particle Data Book and the bottom a simulation of the planned experiment with 20000 charged current  $\nu_\mu$  interactions with the statistical errors shown. Points with errors from the CCFR group at 75, 110, and 210 GeV have been plotted on lower scale to show the relative errors.

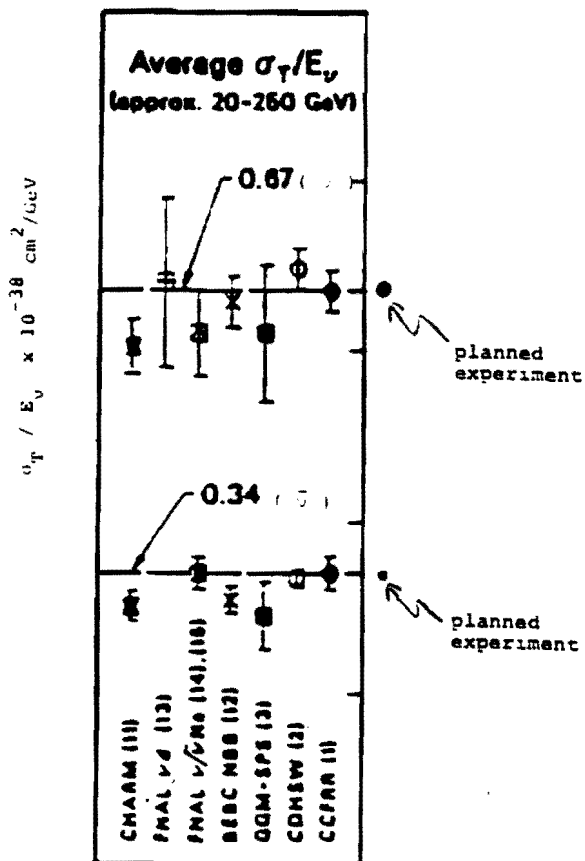


Fig. 7. A comparison of the determination of the slope  $\alpha = \sigma_\nu/E_\nu$  for the planned experiment to previous world data. The top plot is for neutrinos and the bottom is for antineutrinos each with 20000 charged-current interactions. The dots outside the graph represent the planned experiment; the size of the dots are the statistical errors, arbitrarily doubled to reflect any potential systematic errors.

## II. Apparatus

### A. Target and Beam Line

This section will describe the apparatus and beam line; we begin with the target and work downstream. None of the precise locations or apertures are critical unless noted. In

order to handle the high rates in the tagging spectrometer, the experiment must run in slow extraction mode. The overall arrangement is given in Fig. 8. We expect the details of the beamline will be similar to the current M Center line constructed for E731;<sup>14</sup> the main differences are that there will be one beam instead of a dual-beam arrangement and that the beam solid angle will be fifty times as large.

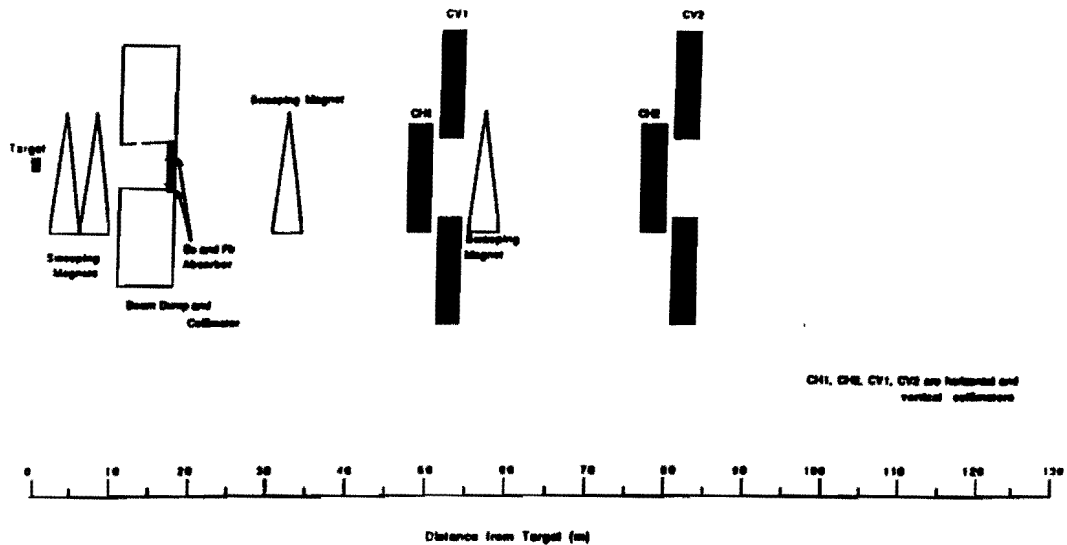


Fig. 8. A schematic of a beam line for the proposed experiment. It is taken directly from the E731 design; the transverse apertures will be approximately a factor of eight larger than in E731 with the z-locations being nearly identical.

The most important change is that the target has been moved to only 260 m. from Lab E. Primary protons must then be transported through the old decay pipe and berm. This difficult task is critical to the experiment: the relative increase in acceptance with the target at the new location is a factor of 25 compared to the present configuration. The design allows

<sup>14</sup>The data on the beamline and the drawing (with adaptations) are taken from M. Woods, "A Search for Direct CP Violation in the  $2\pi$  Decay Modes of Neutral Kaons", PhD Thesis, University of Chicago, 1988 (unpublished)

for 25 m. of shielding before Lab F, which should be adequate for dumping the neutral beam. We will use an instrumented dump both as beam dump and as a muon identifier.

The target will be similar to the one used in previous  $K_L$  experiments at FNAL: 500 mm of Be. A lead plug will be necessary to reduce the photon flux and a Be moderator will be used to adjust the neutron/kaon ratio; we have used a 30 inch Be moderator in our calculations. We have attempted to maximize the rate while maintaining a manageable flux of neutrons and decided that the useful solid angle should extend from -2 to 2 mr in  $\theta_y$  and 2 to 6 mr in  $\theta_x$ . We require variability in  $\theta_y$  of at least 2 mr and in  $\theta_x$  of 0.5 mr in order to "fine-tune" the rates and neutron flux. The calculation uses the parameterization by Malensek of Atherton data for our estimates;<sup>15</sup> this program has been used through several generations of kaon experiments (E533, E584, E617, and E731) and its normalization has been checked to 20%.<sup>16</sup> We have assumed the machine energy will be 900 GeV. If it remains at 800 GeV, we have 20% fewer events; we will then attempt to adjust the targeting angle and moderators to compensate.

The evacuated decay volume begins immediately downstream of the target and will extend 200m. downstream. The pressure must be minimized to prevent neutron interactions in the long decay space: 1 mm. of Hg leads to one interaction every 120 buckets, or about 10 MHz from neutron interactions, and hence a vacuum of a few microns is required. A negligible fraction of our data comes from the first 25 m., and so the final arrangement of collimators, sweepers, absorbers, etc. in this region will not compromise the experiment. The beam will then have a 80 cm full-width at the entrance to the tagger, which will have no hole for passage of the neutral beam. The large beam and "no-hole" configuration is

---

<sup>15</sup>A. Malensek, FN-341.

<sup>16</sup>M. Woods and G. Bock, private communication. The check is based on measured rates in E731.

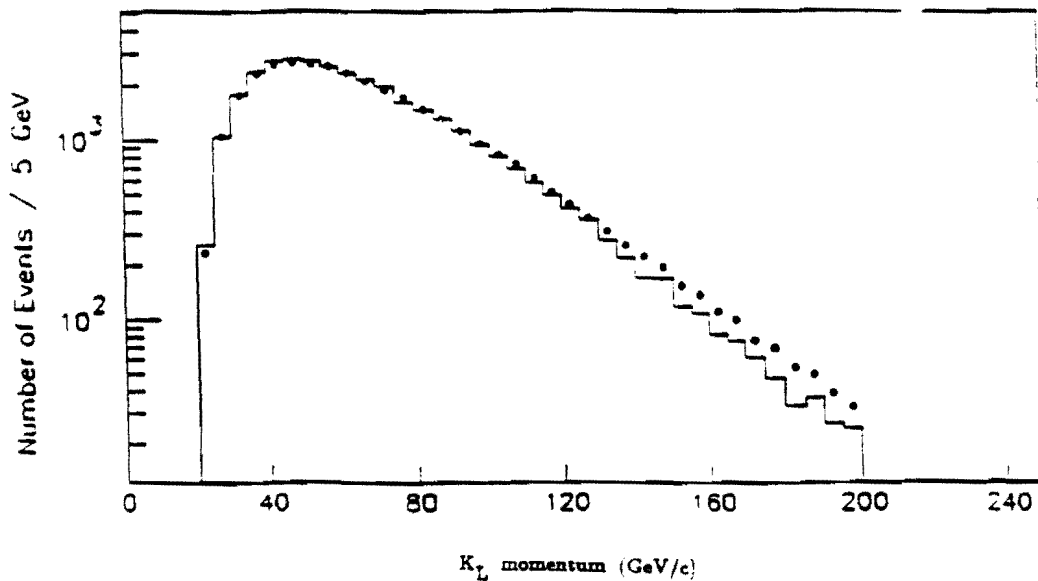


Fig. 10. A comparison of the observed  $K_L$  spectrum in E731 to that predicted by Malensek. The targeting angle for the E731 data was 5 mr, approximately in the center of our targeting. The normalization is checked to 20%; the agreement in shape is excellent.

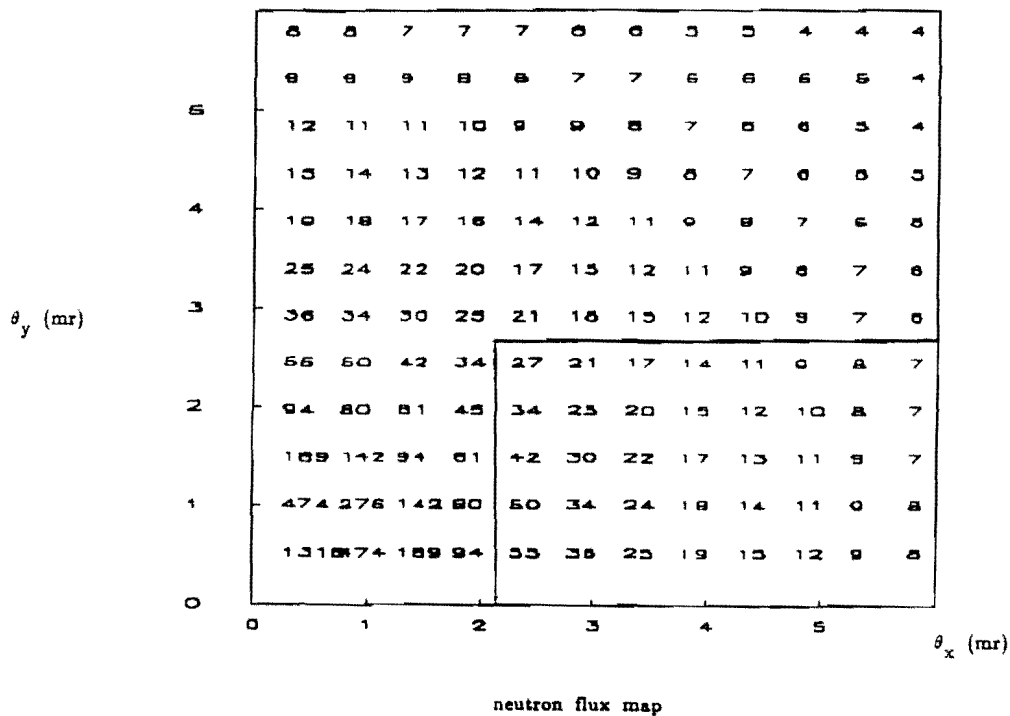


Fig. 11. A flux map for neutrons. The bin size is 0.5 x 0.5 mr, and the normalization is  $10^8/5 \times 10^{12}$  protons. The upper half of the beam is shown. The preferred targeting is symmetric about the horizontal axis. The portion of the beam used is enclosed in the box.

### III. Rates and Acceptances

In this section we explicitly calculate the rates of  $\nu$ -interactions expected in the experiment and the rates from interactions of neutrons and  $K_L$  in the beam; it is an amplification of the information outlined in earlier sections. We request  $2.3 \times 10^{18}$  protons, or 46 weeks of perfect beam time at  $5 \times 10^{12}$  protons per pulse in a 20 sec spill.

As stated earlier, we use the Malensek parameterization for  $K_L$  production; a comparison of the predicted spectrum to the E731 spectrum is given in Fig. 10;<sup>24</sup> the normalization is good to 20%. For neutrons, we use data from the ISR,<sup>25</sup> and for  $\Lambda^0$  production we use a parameterization from the Fermilab hyperon experiments.<sup>26</sup> Figs. 11-14 show flux maps for neutrons,  $\Lambda^0$ , produced  $K_L$  and decaying  $K_L$ , into bins of  $0.5 \times 0.5$  mr. The advantage of large targeting angle in the  $n/K$  ratio is clear: the neutron flux drops by two orders-of-magnitude from 0 to 5 mr while the  $K_L$  flux decreases by only a factor of two. However, choosing a large targeting angle has disadvantages as well: the  $K_L$  are at lower energy and (1) the hadron and lepton are produced at larger opening angle in the lab frame and have a lower geometric acceptance, and (2) the neutrinos are at lower energy and therefore have a smaller cross-section. We have chosen what we consider to be a reasonable compromise between  $n/K_L$  ratio and rate: we have tried to guarantee that rates per wire are under 1 MHz and the space charge for the hottest wire is under  $10^3/\text{mm}^2/\text{sec}$ , and moved to as small a targeting angle as possible consistent with these constraints.

---

<sup>24</sup>M. Woods, op. cit.

<sup>25</sup>J. Engler et al., Nucl Phys B84:70, 1985

<sup>26</sup>L. Pondrom, Phys. Rep. 122, 1985

chambers built at FNAL work extremely well and we have had no significant problem with them. The energy-measuring scintillators are deteriorating, however, and require renovation and repair. It seems the cost of replacing all of the liquid scintillator with acrylic is prohibitive - there are 80 counters, each 3m by 3m. (The photomultiplier tubes are failing and need to be replaced; there are four on each counter, for a total of 320). For timing we would replace every fourth plane of liquid scintillator with acrylic scintillator staves to accurately measure the time of the neutrino interaction and of muon passage to the 10 nsec required; this distance between planes guarantees that even short, electromagnetic showers would be well-timed.

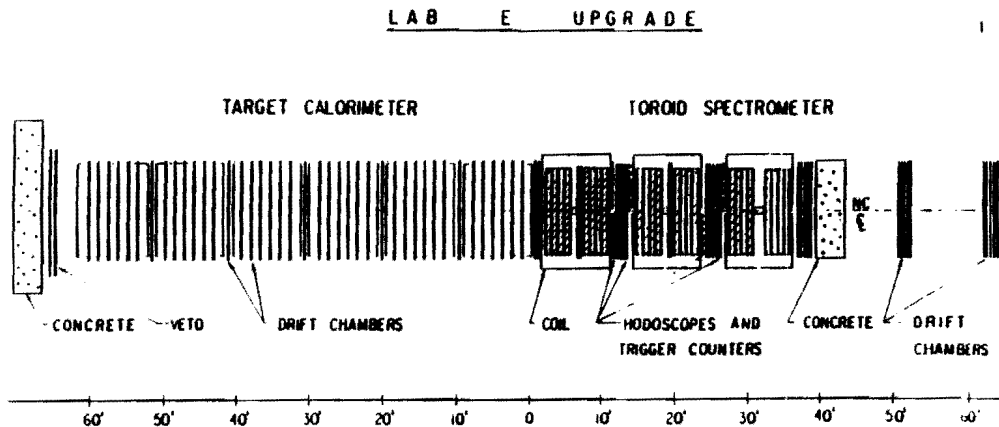


Fig. 9. A schematic of the Lab E neutrino detector. An entering  $\nu$  interacts in the calorimeter, which measures the energy of the interaction and tracks muons. A downstream toroid measures the muon momentum.



oscillation signal from  $\nu_e$  requires *no* muon in the tagger. The loss from punchthrough of  $(\pi e)$  pairs in the data is smaller than 1/8 buckets, since we may demand that the extrapolated track overlaps a struck muon counter. A 4 GeV muon will scatter about 12 cm in 3 meters of steel. If we assume all the electrons from  $K_L$  decay are confined to the beam, (hence overestimating the probability of overlaps with beam-induced showers) the suppression is then (at  $2\sigma$  for scattering)  $(24/80)^2 = 0.18$ , so the total loss of data in  $(0.18)(1/8) = 2.2\%$ .

We *will* have background for the  $\nu_e \rightarrow \nu_\tau$  search if a muon is misidentified as an electron and then misses the muon filter. The probability for a muon missing a dump as a function of momentum, for a 3 meter dump similar to the one planned, was measured in E731<sup>23</sup> and is under 0.3% for muon momenta greater than 20 GeV; our typical lepton energy is 20 GeV or more. Hence for a TRD contamination of  $10^{-3}$ , we expect less than  $3 \times 10^{-3} \times 10^{-3} = 3 \times 10^{-6}$  confusion, or .03 background events in our final sample.

Two planes of scintillators following the dump, in coincidence, will then be the muon signal. By placing more material in between these two planes, we can effectively increase the length of the dump and further reject punchthroughs, which will exit the dump at very low energy. The entire tagger will be 15 m long, with a downstream end 35 m from the upstream wall of Lab E.

### C. Neutrino Detector

We plan to use the CCFR neutrino detector in Lab E (Fig. 9) with only minor changes. It is designed to detect and analyze  $\nu_\mu$  charged-current interactions. The detector has recently been upgraded to use drift chambers with TDC and flash ADC readouts to replace the old spark chambers. The long and reliable history of the detector speaks well for it. The drift

---

<sup>23</sup>G. Gollin, private comm.

tracks extrapolate into the showers. The shorter dead-time of scintillating fibers makes them more attractive than MWPC's for this application; the readout complexity and cost are the disadvantages of fibers. Another, perhaps superior, idea is to use a TRD: typical thicknesses for  $\pi/e$  separation are 2-4%  $\lambda_I$  and 4-6%  $X_0$  with 90% electron efficiency and 0.1% pion contamination.<sup>21</sup> In this case we could keep the number of neutron interactions under 1/bucket; here we are tied to drift chambers and will have to examine the dead times and shower profiles more carefully. One of our major priorities is a test run to determine the details of the calorimeter and to measure the efficiency and rejection power of the device. For example, we need to determine the optimum length of the TRD, where we are trading pion rejection against the number of extra hadron showers.

The first level will not separate pions from muons. A muon filter will serve as both a beam dump and a separator for pions and muons. Our beam Monte Carlo tells us there are 12.5 neutrons/bucket in the beam, and we know from E744/E770 hadron test data that the probability of producing a muon of more than a few GeV/c is less than  $10^{-2}$  for hadron energy of about 450 GeV. Since the rate falls rapidly with energy (about an order of magnitude between 450 GeV and 100 GeV), the higher-energy neutrons in the beam provide the majority of the rate<sup>22</sup> and the contribution for the  $K_L$  portion of the beam is small. Hence we expect a muon to exit the dump once every  $(12.5 \text{ neutrons/bucket} \times 10^{-2} \mu/\text{neutron}) = 1/8$  buckets.

A muon punchthrough does not provide background for the  $\nu_e \rightarrow \nu_\tau$  search since the

---

<sup>21</sup>There are a variety of excellent papers on TRD's. We have used typical values from Fabjan et al., NIM 185(1981) 119; Other papers are De Marzo et al., NIM A253(1987) 235; Denisov et al., FNAL-Conf-84/134-E (presented by A.V. Kulikov), which describes the E715 TRD.

<sup>22</sup>Muoproduction in showers is responsible for about 1/3 of the "same-sign" dimuon background, and hence has been carefully estimated by CCFR and measured in test runs. Estimates from E379 test run data can be found in Lang, op. cit. and punchthrough probabilities based on more detailed studies from E744 were published in Merritt et. al., NIM A245:27, 1986.

shower will not develop significantly. A typical neutron interaction at a few hundred GeV or more will produce a relatively collimated cone of approximately one dozen particles.<sup>20</sup> This should not normally interfere with the particle tracks, determined in six chambers for each view. Assuming one dozen dead wires per interaction (probably a worst-case: note that here we have assumed as many wires as possible are dead, and in calculating space-charge, we have assumed the shower is concentrated on only one wire), and that a struck wire remains dead for five buckets (100 nsec), we expect a loss of no more than 5% of the data from spatial overlaps of tracks and showers.

The magnet will be a large air-gap dipole, 2.5 m. by 2.5 m. to match the chambers. The  $p_T$  kick will be only 500 MeV/c; this relatively small value is adequate for our requirements on momentum resolution.

Separating  $Ke_3$  from  $K\mu_3$  decays can be achieved by first distinguishing electrons from pions and muons and following that apparatus with a muon filter to identify muons. The  $\pi/e$  separation need not be perfect because the critical separation is between the electron ( $Ke_3$ ) and a muon ( $K\mu_3$ ); if electrons and pions are misidentified the event will not look like either a  $Ke_3$  or  $K\mu_3$  decay and will then be rejected, a small loss for any reasonable arrangement. One possibility is to use a segmented calorimeter instrumented with either scintillating fibers or MWPC's to determine the longitudinal and transverse shower spread. Using a high-Z material such as tungsten is advantageous because the ratio of radiation lengths to interaction lengths is thirty; hence we expect 2.5 interactions/bucket for a 10%  $\lambda_I$  calorimeter. These showers will be highly collimated and we can further reject them by demanding the particle

---

<sup>20</sup>J. Elias et al., Phys. Rev. D22(1980) 13. This reference provided data from the Fermilab SAS for pC interactions at 50, 100, and 200 GeV. We have assumed that neutrons and protons behave identically, logarithmically fitted their multiplicity, and extrapolated to 900 GeV; the mean neutron energy in our solid angle is 450 GeV.

kaon flux is nearly flat over the solid angle; hence, the rate is  $(6.25/200)\text{MHz} = 31 \text{ KHz}$ . The neutron flux is more concentrated: the hottest 10% of the wires see  $1/3$  of the rate, implying  $(6.25 \text{ MHz} / 20 \text{ wires} \times 1/3 \text{ rate}) = 0.1 \text{ MHz}$ . The sum of neutrons,  $K_L$  interactions, and  $K_L$  decays is then  $0.5 \text{ MHz}$  in the worst case. For calculating dead times, let us assume a hadronic interaction populates the entire cell; hence the wire will be dead for the time it takes to drift from the nearest field wire into the sense wire  $= (2\text{mm}/(50\mu/\text{nsec})) = 400 \text{ nsec}$  dead time per hit. Tracks from  $K_L$  decay will deaden the wire for approximately  $100 \text{ nsec}$ . Hence the dead time in the hottest wires will be about 5% from each source, or 10% total. A typical wire will be dead about 5% of the time. With three chambers before and three after the magnet in the bend direction, and six in the non-bend, and two offset planes per chamber, we do not expect a significant problem with pattern recognition.

We also need to consider the space charge produced. Here, the typical multiplicity of 12 particles/interaction (as explained below) increases the relative importance of interactions dramatically. The space charge in the hottest 10% of the wires from neutron interactions is  $(6.25 \text{ MHz} \times 12 \text{ particles/interaction}/(0.4 \text{ cm} \times 80 \text{ cm} \times 20 \text{ wires}) \times 1/3 \text{ of the rate}) = 4.0 \times 10^2 \text{ particles/mm}^2/\text{sec}$ . If more detailed design and chamber testing indicates this is unacceptable, we could deaden a small region of the chambers with a negligible loss in acceptance, since the  $K_L$  decay products are almost uniformly spread over the chambers. The conclusion is that a 4 mm wire spacing leads to manageable rates and space-charge effects. These estimates have a large "safety-margin" since they are for the worst-case and even these deliberately pessimistic estimates are acceptable.

Although the rate from legitimate  $K_L$  decays dominates the neutron and kaon interaction rate, we wish to minimize the number of hadronic interactions in the spectrometer so that the events will be as clean as possible. Since the number of interaction lengths is so small, the

downstream of a large dipole (with two staggered x-planes and two y-planes per station): 200 wires then cover the 80 cm. beam. It is certainly possible to increase the spacing outside the beam and reduce this number by a factor of two. We have carefully calculated the total amount of material in the spectrometer, including vacuum windows, chambers, Helium, etc. and believe 1.0% of a interaction length is achievable, which we calculate as follows. The 4 ft. by 4 ft. window of E617 used 30 mil-equivalent of Mylar; our 2.5 m by 2.5 m window has four times the area, and therefore must be at least 125 mils thick. This yields 0.5%  $\lambda_I$ . The chambers have 4 mils of Kapton for windows, which double as ends of He bags. The gas is taken to be 50/50 Ar/Ethane at 1 ATM, 1.5 in. thick. Each chamber has two x planes, two y planes, and two ground planes of  $100\mu$  thick tungsten wires spaced 4 mm apart. The sum is then  $2.2 \times 10^{-4}$ /chamber; we conservatively round up to  $3 \times 10^{-4}$ /chamber for calculations. The sum of windows and chambers is then 0.8%  $\lambda_I$ . The space between chambers is filled with He to minimize interactions and multiple scattering and contributes a negligible amount to the sum. We therefore believe 1.0%  $\lambda_I$  is a reasonable estimate.

A 4 mm spacing and 1%  $\lambda_I$  imply that no wire will see more than 0.5 MHz: this is in the hottest portion of the beam and includes neutron and kaon interactions in windows and the spectrometer itself, along with the kaon decays in the beam. The rate of kaon decays is 75 MHz and we expect 12.5 neutrons and an equal 12.5  $K_L$ /bucket in the beam. Our simulation tells us that roughly 50% of the tracks from charged decays enter the spectrometer; conversions of photons from  $K_L \rightarrow 3\pi^0$  decay in the spectrometer are an unimportant contribution. Under these assumptions, the average rate per wire from all  $K_L$  sources is  $(75 \text{ MHz} \times 2 \text{ tracks/decay} \times 0.5 \text{ acceptance/track}/200 \text{ wires}) = 380 \text{ KHz}$ . We calculate the rate from neutron and  $K_L$  interactions as follows: at 25 hadrons/bucket, 1%  $\lambda_I$  implies one interaction every four buckets, or 12.5 MHz from interactions (half neutrons, half  $K_L$ ). The

event per 50K  $\nu_e$  tags is achievable. This includes an order-of-magnitude suppression from timing information: at 1.5  $K_L$  decays/rf bucket, our expected rate, we may calculate the probability that a  $Ke_3$  and  $K\mu_3$  decay will occur in the same bucket and that the leptons will have the same sign: this time-coincidence occurs in only 10% of all  $Ke_3$  decays. This factor of ten is critical to adequate background rejection and it is therefore imperative that we obtain timing in both the tagger and the neutrino detector to the nearest bucket; 10 nsec seems an appropriate and achievable goal.

The particle tracks must be reconstructed with high precision in order to reconstruct the kaon vertex - 250 $\mu$  resolution will be necessary. This demands we use drift chambers rather than MWPC's. The planned chambers are 2.5 m by 2.5 m - to obtain 250 $\mu$  resolution would require a little under 1 mm wire spacing in MWPC's, which has never been achieved in chambers of this size. We have assumed 4 mm wire spacing is manageable. Chambers of a similar size (2 m square) and wire spacing (3mm) have been constructed in the past, although run as MWPC's;<sup>18</sup> these chambers are now being used by E665. The primary problem is wire oscillations caused by electrostatic forces, which is solved by a now-standard method of supports. Our expected "worst-case" space-charge will be less than 10<sup>3</sup>/mm<sup>2</sup>/sec, which will produce at most a small loss of efficiency.<sup>19</sup> We therefore expect the design and operation of the planned chambers is possible, although they certainly will demand care and precision.

Our goal is to keep the rate per wire as low as possible. The entire system will have about 15K sense wires if the spacing is a uniform 4 mm., three chambers upstream and three

---

<sup>18</sup>M. DePalma et al., NIM 217 (1983),135

<sup>19</sup>(S. Wolbers, priv. comm.) Research into chamber gases is probably warranted. An excellent article on high counting rate chamber gases is Fischer et al., NIM A238 (1985),249.; they have operated small chambers at several times 10<sup>5</sup>/mm<sup>2</sup>/sec.

forced by the requirement of adequate statistical power in the experiment: the neutrino cross-section is a powerful constraint! The decay pipe will be terminated by a thin window, probably Mylar/sailcloth, in order to minimize multiple scattering. It will be important to track the decay products backwards to the decay point and scattering in this plane will obviously degrade the vertex resolution.<sup>17</sup>

## B. Spectrometer

The spectrometer has two functions: first to identify that a decay has occurred and to measure the time of the decay as accurately as possible, and second to distinguish  $Ke_3$  from  $K\mu_3$  decays.

These goals require careful design. As will be shown in the next section, the spectrometer must handle rates of roughly one decay/rf bucket (2 nsec wide every 18.8 nsec). This high interaction rate places constraints on the detector; we will attempt to accurately predict the experimental environment and calculate fluxes so that we are sure that each part of the detector is capable of its task.

The high rate also demands that we use the tagging spectrometer to momentum-analyze and track both the lepton and the hadron from the kaon decay back to a vertex; then the location and energy of the neutrino in the neutrino detector predicted from momentum balance can be compared to the measured neutrino energy and impact point in the neutrino detector in order to reject background. We have simulated the rejection power of the system, using calculated resolutions for the proposed dipole spectrometer and measured resolutions in the CCFR neutrino detector. The studies indicate that a background of fewer than one

---

<sup>17</sup>A similar window for E617 contained .0025 radiation lengths, and we have scaled for the greater diameter of the window for this experiment. The resultant thickness of 1% of a radiation length is adequate for the vertex resolution required, although we would like to make this window as thin as safely possible.

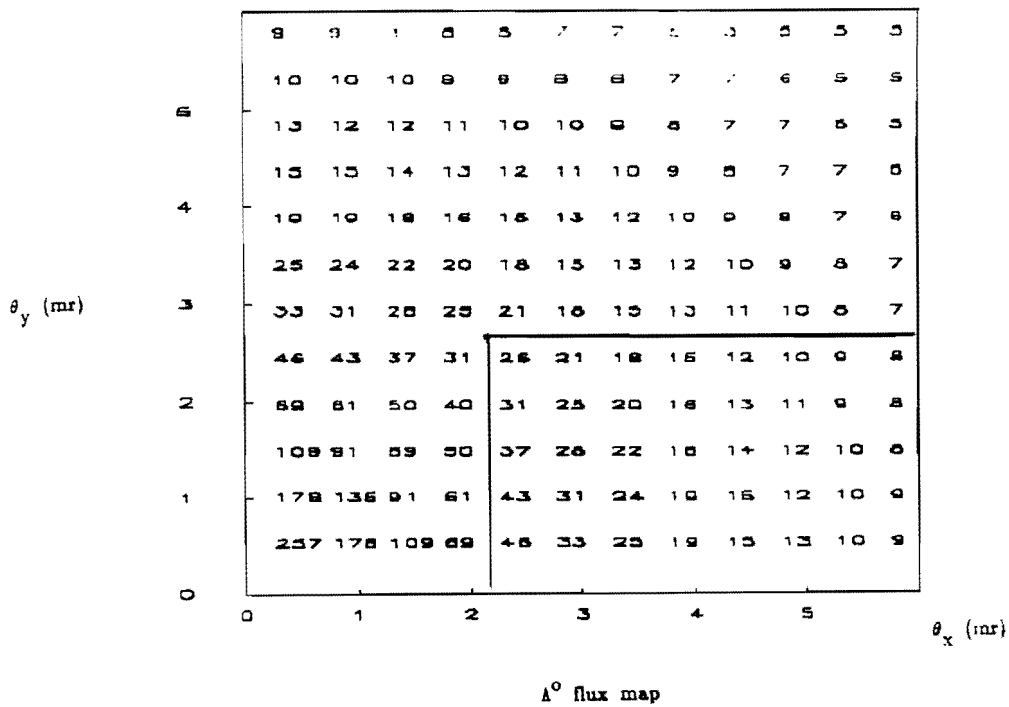


Fig. 12. A flux map for  $\Lambda^0$ , otherwise the same as Fig. 10.

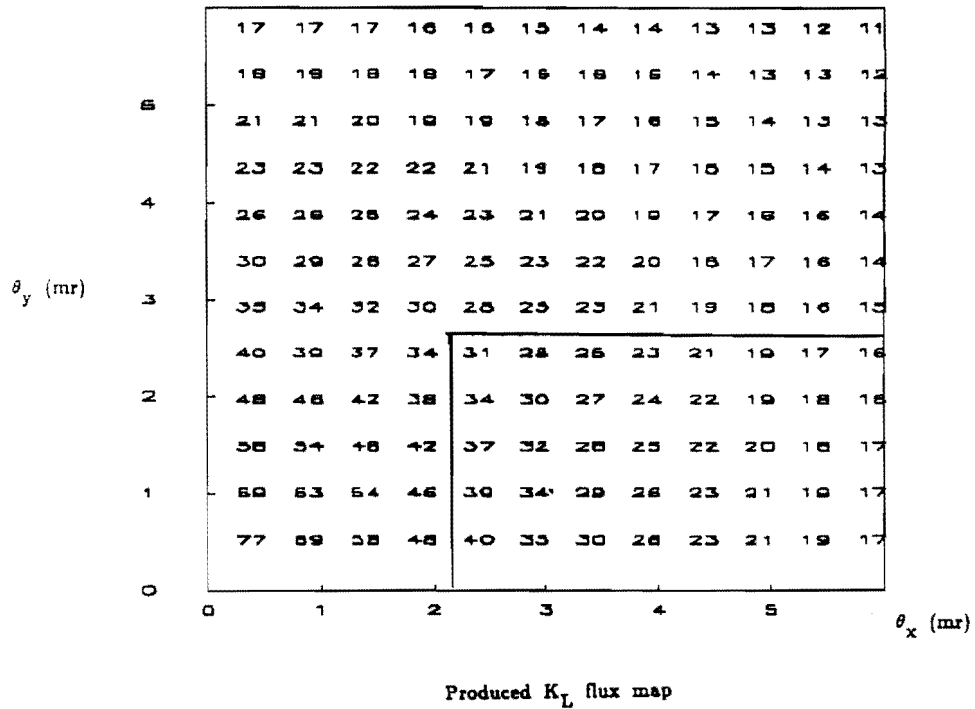


Fig. 13. A flux map for produced  $K_L$ , otherwise the same as Fig. 10.



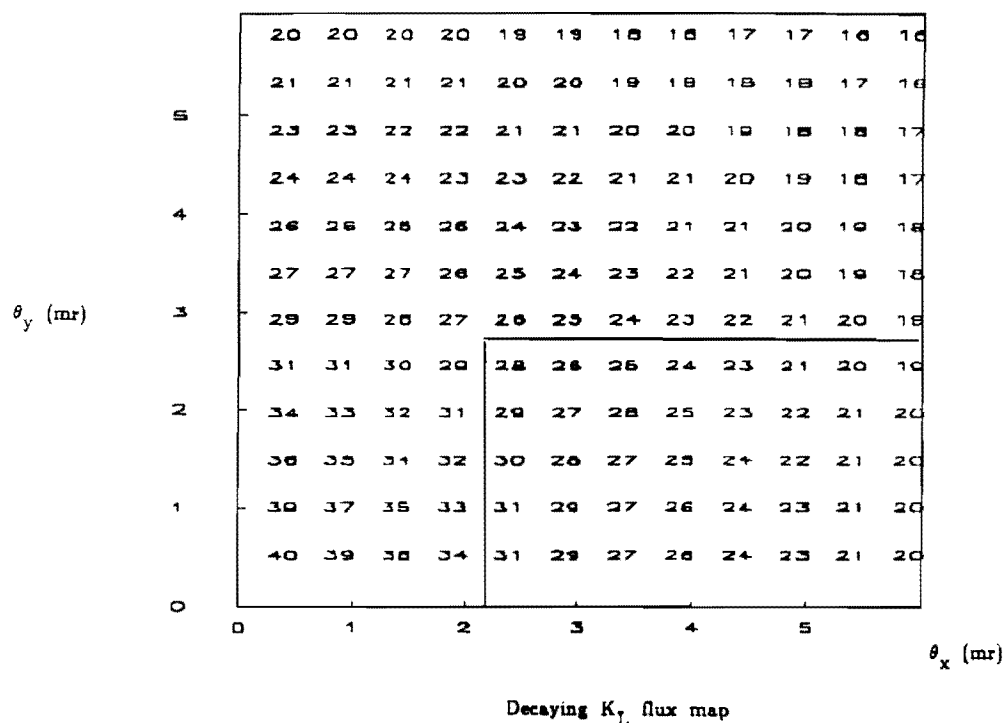


Fig. 14. A flux map for decaying  $K_L$ , with a normalization  $10^6/5 \times 10^{12}$  protons.

The final chosen angle is  $-2$  to  $+2$  mr in  $\theta_y$  and  $+2$  to  $+6$  mr in  $\theta_x$ . We would like up to 2mr variability in  $\theta_y$  to allow for errors in our estimates. We have placed 30 in. of Be and  $10X_o$  of Pb in the beam to further moderate the  $n/K_L$  ratio and absorb photons in the beam; both these moderators will be variable to adjust to real conditions, but the rates are approximately correct and the choice of moderators and their lengths are consistent with previous choices in the M Center line. We then find, using our flux tables,  $1.25 \times 10^{10}$  neutrons, a similar  $1.25 \times 10^{10} K_L$ , and  $1.5 \times 10^9$  decaying  $K_L$  per spill. The mean  $K_L$  energy is 70 GeV/c, with a spectrum similiar to that of Fig. 11. The  $\nu$  energy spectrum, weighted for cross-section, is shown in Fig. 15.

We use the flux of  $K_L$  into each unit of solid angle, with the correct momentum spectrum

for that angle, to calculate a geometric acceptance of 14.8% for the tagger/neutrino detector pair ( a hole for passage of the neutral beam would reduce this number by an order-of-magnitude). The mean neutrino energy is 47 GeV/c, and the probability of interaction in the CCFR detector is  $2 \times 10^{-11}/\text{GeV}$ . With the resultant spectrum of neutrinos and with standard CCFR fiducial cuts ( $p_\mu > 9 \text{ GeV}/c$  at the vertex, and geometric acceptance), we have calculated an acceptance of 0.8 for muons from charged current  $\nu_\mu$  interactions. The lower energy muons from  $\tau$  decay, from the chain  $\nu_\tau N \rightarrow \tau X$ ,  $\tau \rightarrow \mu\nu\nu$ , have an acceptance of 0.67. Our total sample before cuts is then:

$$\begin{aligned}
 \#(\nu + \bar{\nu}) &= \\
 & (1.5 \times 10^9 K_L/\text{spill}) \times \\
 & (.148 \text{ acceptance}) \times \\
 & (0.8 \text{ CCFR acceptance}) \times \\
 & (47 \text{ GeV} \times 2 \times 10^{-11}/\text{GeV}) \times \\
 & [0.39 BR(K_L \rightarrow \pi e \nu_e) \text{ or } 0.27 BR(K_L \rightarrow \pi \mu \nu_\mu)] \times \\
 & 4.6 \times 10^5 \text{ spills} \\
 & = 30,000(\nu_e + \bar{\nu}_e) \\
 \text{and} \\
 & = 20,800(\nu_\mu + \bar{\nu}_\mu)
 \end{aligned}$$

The application of cuts to eliminate background will be covered in the next section. The cross-section sample will be cut by only 20% but the  $\nu_e \rightarrow \nu_\tau$  oscillation sample will be cut

in half.

The  $\Lambda^0$  flux is a potential problem, both from extra rate in the spectrometer and the decay chain  $\Lambda \rightarrow p\pi^-$ ,  $\pi \rightarrow \mu\nu_\mu$  where the  $\nu_\mu$  hits the neutrino detector. We have simulated the  $\Lambda^0$  spectrum and determined that within our targeting region there are approximately 10  $\Lambda^0$  produced per bucket with a mean lifetime of 70-80 cm. The decay products can then be easily swept out of the beam. The background contribution of the  $\nu_\mu$  from the above decay chain with *no* sweeping and standard cuts (fiducial volume and  $E_\nu > 30$  GeV) is  $1/10^6$  events and is hence negligible. There are two  $\Lambda^0$  rare decay modes which must be considered as well:  $\Lambda^0 \rightarrow \pi e \nu_e$  (BR =  $8.3 \times 10^{-4}$ ) and  $\Lambda^0 \rightarrow \pi \mu \nu_\mu$  (BR =  $1.57 \times 10^{-4}$ ). The first decay, into  $\nu_e$ , will not contribute background to the oscillation searches but only to the cross-section studies. The contribution to the cross-section after acceptance cuts will be under  $10^{-5}$  of the signal. The second, which produces  $\nu_\mu$ , is a potential background. After acceptance and reconstruction cuts the background is at a similar, negligible level.

Similarly, production of  $\pi/K$  and background contribution from their decays are small.  $K_S$  decay has been modeled as well, and *before* sweeping, contributes 1 background event from  $K_S \rightarrow \pi^+\pi^-$ ,  $\pi \rightarrow \mu\nu_\mu$ . However, 99% of the  $K_S$  decay in the first 50 meters and after sweeping we expect no background from  $K_S$ .

Finally, we consider “bare-target” production: production of charged  $\pi$ ,  $K$  and their decays into  $\mu\nu$ . The neutrino trigger will require  $E_\nu > 20$  GeV: for this energy, the  $\pi$  lifetime is 1.12 km and the  $K$  lifetime is 150 m. With enough sweeping to dump 900 GeV primary protons in the first ten meters, we do not expect a significant bare-target background, since higher-energy (longer-lived) particles will have progressively less chance to decay. A TURTLE simulation to systematically calculate the rates will be performed as part of a

detailed beam-line design.

#### IV. Triggering

The experiment will trigger on total energy deposit in the neutrino detector. Our data sample for simulations was cut at 30 GeV; we propose to have an  $E_H$  (hadronic energy) trigger of at least 20 GeV in the scintillation counters in coincidence with the RF. Cosmic ray air showers will dominate the trigger rate and from CCFR data with an  $E_H$  cut of 20 GeV we expect a trigger rate of 1-2 Hz.

We can generate an RF signal with scintillators near the target: they will see the beam bunches and we can then generate an RF signal which will be sent to the tagger and the neutrino detector. The trigger will then demand that the  $E_H$  trigger be in time with the upstream scintillator. The tagger, unlike the neutrino detector, will not be used in the trigger: the tagger readout will only encode the time of an interaction for each active channel of the spectrometer. In the 500-750 nsec that it will take for the neutrino to travel from the tagger to the neutrino detector, for the electronics to make a trigger decision, and then send a trigger back to the tagger, any channel will have less than 1.0 hit on average (since the rate per wire is only 0.5 MHz in the worst case). Each readout channel could store the time and location of any hits with a memory 1  $\mu$ sec deep; fewer than 7500 hits would then need to be processed (at the highest rate of 0.5 MHz, in 1  $\mu$ sec, half the wires would be hit). We could conceivably put mean-timing circuits on pairs of adjacent wires to only accept hits in time with the neutrino interaction, along with any unpaired hits, to reduce the amount of data to be processed.

## V. Backgrounds and Systematic Errors

In this section we will discuss the backgrounds to the oscillation signals. First, we cover the physics of the sources; second, we will describe the reconstruction algorithm, and third, use the algorithm and predicted resolutions to set cuts and determine the contaminations. We conclude with a discussion of the systematics and backgrounds for the  $\nu_\mu \rightarrow \bar{\nu}_\mu$  search and the cross-section sample.

A potentially serious background in  $\nu_e \rightarrow \nu_\mu$  or  $\nu_e \rightarrow \nu_\tau$  searches arises from mistags, depicted in Fig. 16. A mistag can occur whenever a  $Ke_3$  and a  $K\mu_3$  decay occur within the time resolution of the system; with 10 nsec time resolution, we only accept decays within the same RF bucket. Then if the  $(\pi\mu)$  pair escapes detection and the  $(\pi e)$  pair is accepted, but the  $\nu_\mu$  interacts, we will have an oscillation signal. This background may be simulated in a straightforward way: generate  $Ke_3$  and  $K\mu_3$  decay pairs, look for the proper pattern, and then apply the reconstruction algorithm to accept or reject the event. The case in which all the tracks enter and the neutrino is associated with the incorrect ( $\pi$ -lepton) pair provides a negligible contribution and we ignore it.

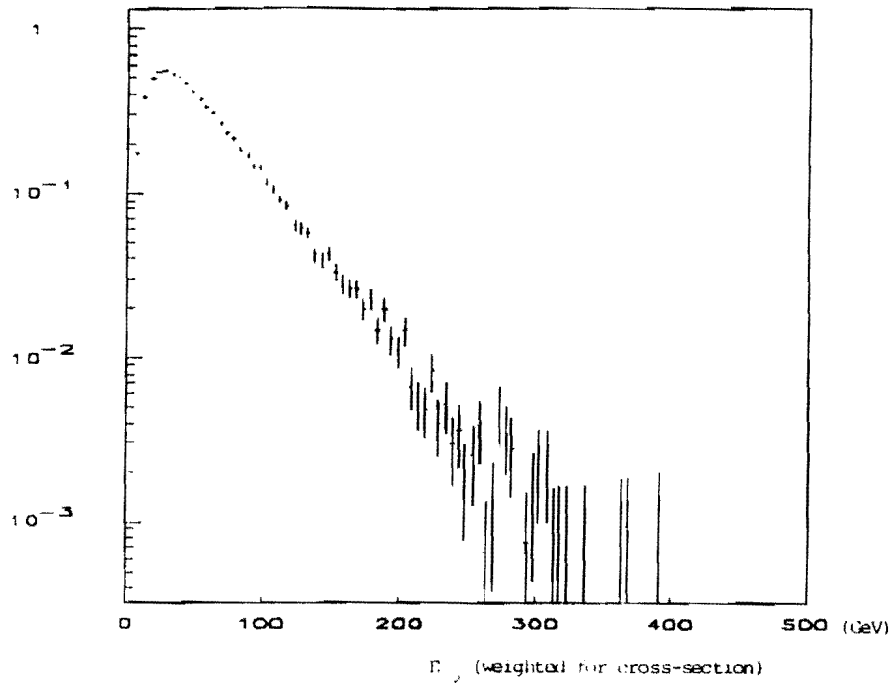


Fig. 15. The spectrum of  $\nu$  incident on the detector, weighted for the energy dependence of the cross-section.

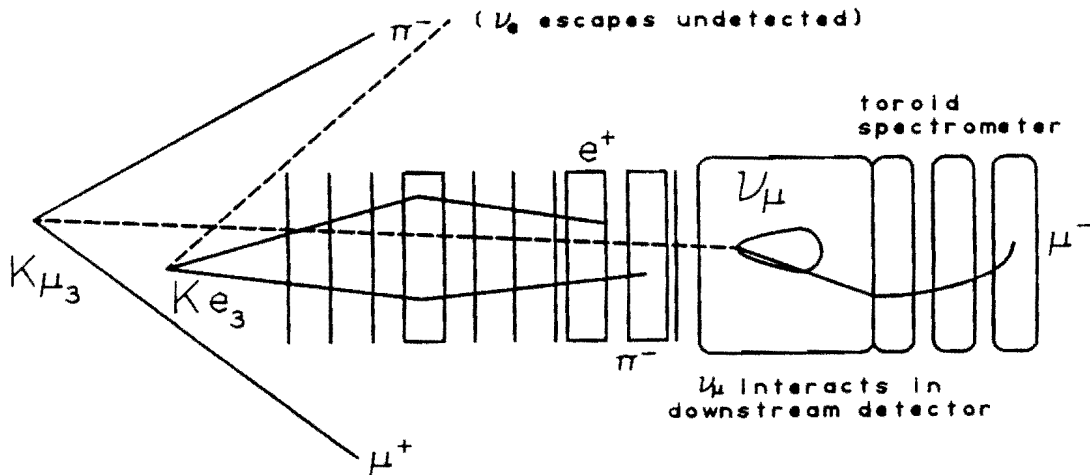


Fig. 16. A schematic of a mistag. A  $Ke_3$  and a  $K\mu_3$  decay occur simultaneously. The  $\nu_\mu$  from the  $K\mu_3$  interacts, the  $\nu_e$  escapes or does not interact in the neutrino detector. With the  $(\pi e)$  pair tagged as shown, the combination appears to be an oscillation.

The rejection factor has two terms: the first comes from the probability of two or more decays occurring in the same bucket. This is a straightforward calculation in Poisson statistics: at our rate of 1.5  $K_L$  decays/bucket we find 8.4% for the overlap where both the electron from  $Ke_3$  and the muon from  $K\mu_3$  have the same charge. If they do not have the same charge, the "coincidence" with the neutrino detector will not appear to be an oscillation.<sup>27</sup> The second, larger rejection, comes from the reconstruction of the  $K_L$ , which we now examine in detail.

The dipole spectrometer will reconstruct the momentum vectors of the pion and lepton. We then project the tracks back to a common vertex and determine a three-dimensional decay point for the  $K_L$ . The chambers are assumed to have a gaussian  $250\mu$  position resolution and we assume gaussian multiple coulomb scattering in the vacuum window (1% rl). The resultant deviations in the decay vertex are shown in Fig. 18 and Fig. 19; the first plot is the error in the x- or y- transverse position and the second shows the error in reconstructed position along the beamline. We then take the position of the target and draw a line from it to the decay vertex. This line provides the initial direction of the  $K_L$ .

---

<sup>27</sup>Except for a special case: Let us posit a  $(\pi\mu^+)$  pair which escapes, a  $(\pi e^-)$  in the tagger, and a  $\nu\mu$  neutral-current interaction in the neutrino detector which then produces an "opposite-sign" dimuon from charm decay. This background is suppressed by 1/3 for the neutral current cross-section and a factor of 400 for the "opposite-sign" rate before reconstruction and timing cuts.

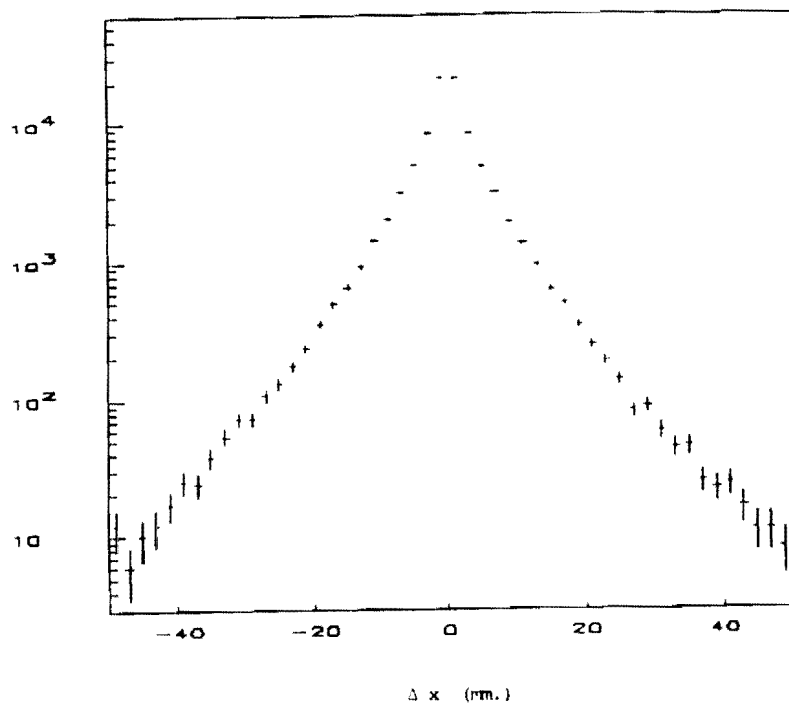


Fig. 17. The difference in the x-coordinate of the reconstructed vertex from the true value. The distance is given in mm.

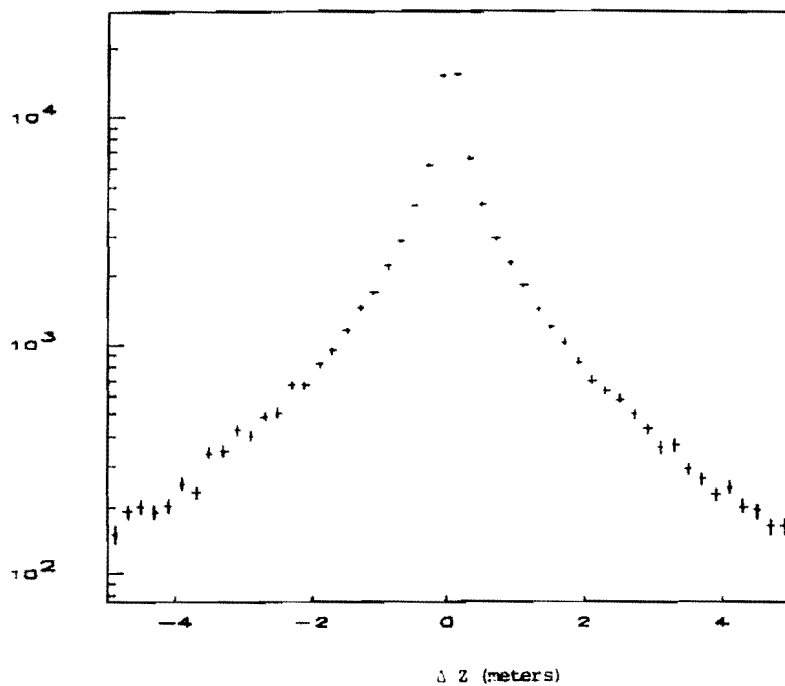


Fig. 18. The difference in the z-coordinate of the reconstructed vertex from the true value. The distance is given in meters.



At this point we have the momenta and trajectories of two of the daughter particles (but not the neutrino) and the initial trajectory of the  $K_L$ . We do *not* have the momentum of the  $K_L$  since that would require knowledge of the neutrino momentum vector. We may now reconstruct the  $K_L$  up to a two-fold ambiguity in its energy. Fig. 19 shows the difference of the two solutions divided by their sum; we see the difference is normally quite small but extends to large values. Taking each solution in turn allows us to predict two possible momentum vectors for the neutrino: two pairs of neutrino energy and transverse impact point in the neutrino detector. We then *compare* each pair to the measured values. Fig. 20 shows the smaller difference in transverse position [ $\Delta r = (\Delta x^2 + \Delta y^2)^{\frac{1}{2}}$ ] for each of the two pairs (the neutrino detector has a vertex resolution of 1.3 cm. for each of x,y). Having made this choice, we then plot the energy resolution  $\Delta E_\nu/E_\nu = (E_{\nu, \text{measured}} - E_{\nu, \text{predicted}})/E_{\nu, \text{predicted}}$  (the energy resolution of the neutrino detector is given by  $\Delta E/E = 0.89/\sqrt{E}$  for the hadronic shower and  $\delta p_\mu/p_\mu = 0.11$ ) in Fig. 21. We see the position determination is reasonable but the energy resolution does not provide as stringent a test, largely because of the poor energy resolution of the neutrino detector.

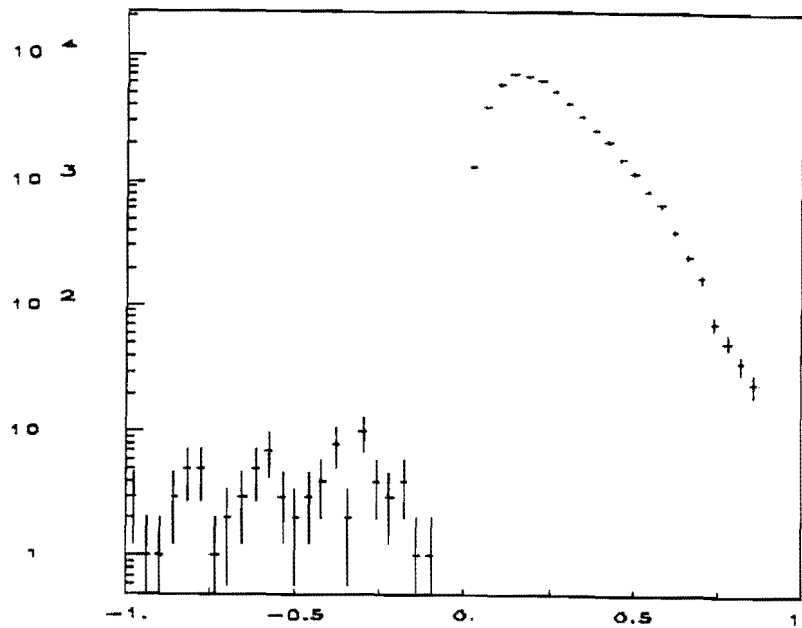


Fig. 19. The value of the  $K_L$  momentum is determined up to a two-fold ambiguity. Here we plot  $(p_1 - p_2)/(p_1 + p_2)$ ; for physical events, we have chosen  $p_1 > p_2$ . The negative tail arises from resolution smearing.

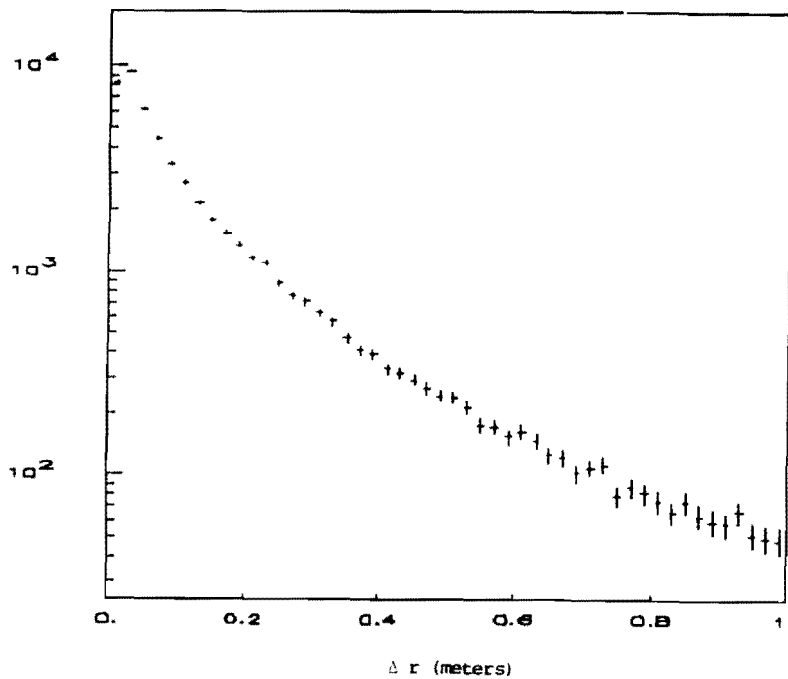


Fig. 20. The difference in distance from the reconstructed impact point in the neutrino detector to that predicted from the tagger. The distance is given in meters.

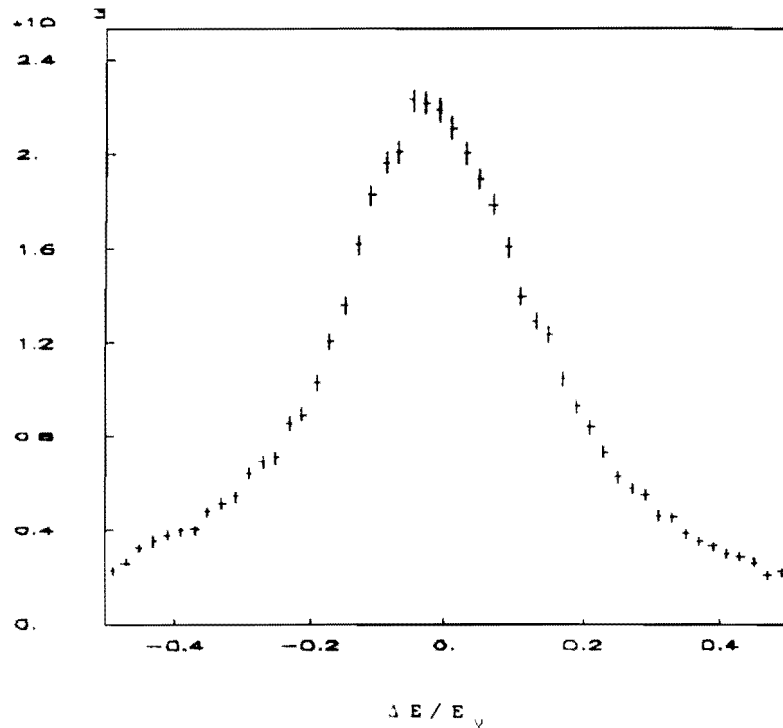


Fig. 21. The difference in neutrino energy predicted from the tagger from the measured value, divided by the predicted value.

There is an additional problem with the energy determination which we suspect makes it unusable for background rejection in the  $\nu_e \rightarrow \nu_\tau$  search. There is normally approximately 5-10% "missing energy" - energy which escapes detection largely in the form of neutrinos created in the shower. The CCFR group has measured this in the Lab E detector and we could certainly apply a correction, which would be adequate for  $\nu_e \rightarrow \nu_\mu$  and  $\nu_\mu \rightarrow \bar{\nu}_\mu$  studies. However, for the  $\nu_e \rightarrow \nu_\tau$  search, there are two missing neutrinos from  $\tau \rightarrow \mu\nu\nu$ . This will smear the energy resolution so as to be largely unusable (certainly we could cut on the visible energy being much *larger* than the predicted energy, and we will probably eventually use that). In order to avoid the resultant problems and complexities, for the  $\nu_e \rightarrow \nu_\tau$  oscillation studies we will quote results using *only* the transverse agreement.

We see a long tail in the position resolution plot which extends to surprisingly large values

of  $\Delta r$ . The source of this tail is the ambiguity in the  $K_L$  reconstruction and arises from a mismeasurement of the initial  $K_L$  direction. The error occurs predominantly for decays at small distances from the target. If the vertex resolution (which worsens as the decay moves upstream) is large compared to the beam size, the initial  $K_L$  direction will have large errors and hence the reconstruction will be wrong. A second contribution comes from the finite target size, and again is worse for decays far upstream. This error in reconstruction is the reason we must lose approximately half the data in order to reduce the background to less than an event.

We first describe the background calculation for the  $\nu_e \rightarrow \nu_\tau$  search. We may compare the plots of  $\Delta r$  for the correct  $Ke_3$  pair to randomly generated  $K\mu_3$  decays, both of which populate the neutrino detector evenly. We require  $\Delta r < 15$  cm. and find 0.3 background events after all cuts (acceptance, reconstruction, and timing; in addition we have placed a cut on the  $p_T$  of the  $\mu$  with respect to the hadron shower direction, which will be discussed later and assumed 0.9 electron efficiency in the particle identifier). The  $(\nu_e + \bar{\nu}_e)$  sample is reduced to 16K from 30K. The rejection factors break down as follows:

I.	Poisson statistics @ 1.5 $K_L$ decays/bucket	0.084
II.	Probability of $(\pi\mu)$ escaping, $\nu_\mu$ hitting	$4.0 \times 10^{-2}$
III.	Probability of $(\pi e)$ acceptance in tagger	0.23
IV.	Probability that $(\pi e)$ matches $\nu_\mu$	$4.2 \times 10^{-3}$

A final suppression arises because the  $\nu_\mu$  accepted in II. above have a mean energy of 27 GeV (the true matches have an mean  $E_\nu$  of 47 GeV). We then calculate the number of background events exactly as we calculated the number of signal events at the end of section III. A more refined calculation is probably unjustified: for example, we have not simulated non-gaussian tails in the resolutions. However, the background is clearly small and the answer is approximately correct. We expect to measure the real resolutions from the data and only then will be we able to estimate the mistagged background more accurately.

The second source of background for  $\nu_e \rightarrow \nu_\tau$  is the “same-sign” dimuon signal shown in Fig. 24. This occurs when a  $\nu_e$  interacts and is correctly tagged, but a muon exits from the hadronic shower and survives the acceptance cuts in the neutrino detector. If the muon has the same charge as the muon expected at the vertex, then the event will pass the “charge-matching” requirement and appear to be an oscillation. This background is iden-

tical to the background in the “same-sign” dimuon search of E616 and E744/E770 and has been extensively studied in those experiments.<sup>28</sup> The overall scale is easily calculated: E744 observed approximately 115 same-sign dimuons with  $p_\mu > 9$  GeV/c in a fiducial sample of 780K charged-current  $\nu_\mu$  events. We then expect  $1.47 \times 10^{-4}$  events with  $p_\mu > 9$  GeV/c per charged-current neutrino interaction (neutral current  $\nu_e$  interactions, which look the same topologically, will contribute another 1.2 events), or 3.5 events in our 16K sample. We may then apply kinematic cuts (for example, on the  $p_T$  of the muon with respect to the hadronic shower) and reduce this background by an order-of-magnitude without significant loss in the oscillation sample. We have used the CCFR Monte Carlo to calculate the measured  $p_T$  distribution for shower muons and for muons from  $\tau$  decay: the distribution in  $p_T$  is shown in Fig. 25. With a cut on  $p_T$  of 1.0 GeV/c we find an order-of-magnitude loss in the background with a 15% loss in signal (the cut had been included in the 16K estimate).<sup>29</sup>

---

<sup>28</sup>B.A. Schumm et al., Phys. Rev. Lett. 60(1988), 1618. For more detail see B. A. Schumm, Like Sign Dimuon Production in High Energy Neutrino Interactions, PhD Thesis, University of Chicago (1988) unpublished.

<sup>29</sup>These cuts were not used by E744/E770; the distributions of  $p_T$  and other variables were compared to the simulations of  $\pi/K$  decay in the shower. Since the source of any dimuon excess was unknown, placing cuts could accidentally eliminate the signal and it was therefore safer to examine the entire distribution compared to the  $\pi/K$  background. In addition, the Lab E drift chambers were fitted with FADC's for E770 so that the energy flow of the hadronic shower can be accurately measured. We expect to use them in applying  $p_T$  cuts to eliminate the shower background; for this study, we have used the old analysis without the FADC's and will undoubtedly have greater background rejection with them.

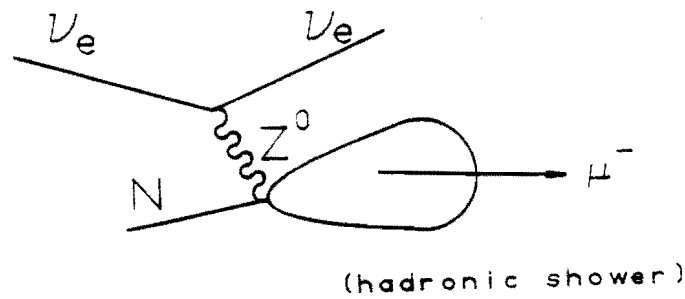
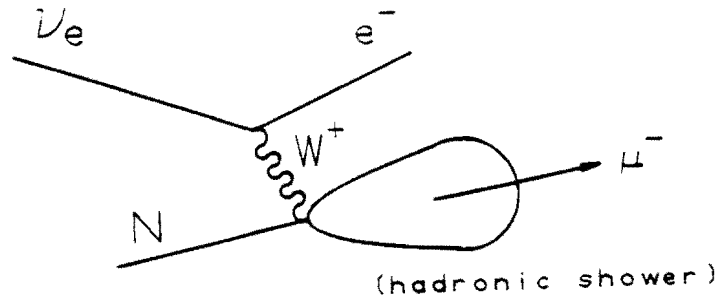


Fig. 22. The source of "same-sign" dimuons. A muon is produced in the hadronic shower. For  $\nu_e$ , we cannot separate charged-current from neutral-current events and hence both diagrams contribute.

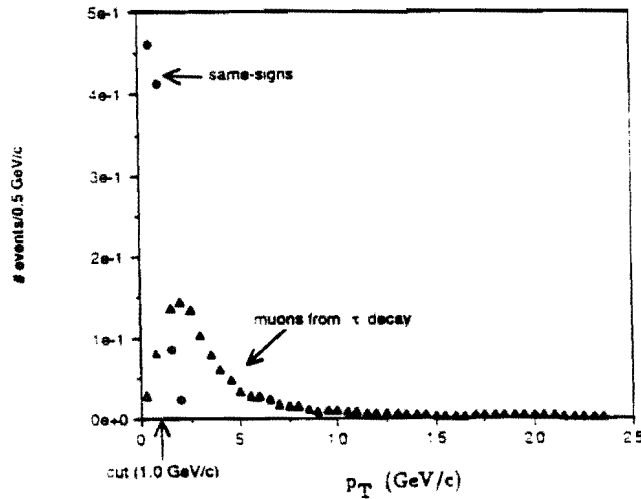


Fig. 23. The  $p_T$  of the muon with respect to the hadron shower. The sources are as shown: one from "same-sign" production, and the other from the final muon in  $\nu_\tau N \rightarrow \tau X$ ,  $\tau \rightarrow \mu\nu\nu$ . The samples have been normalized to 1 event. The cut was placed at 1 GeV/c in the simulation.

The  $\nu_\mu \rightarrow \bar{\nu}_\mu$  sample has, as explained earlier, a background from “opposite-sign” dimuon production. We estimate less than an event from the charged-current sample from the  $p_\mu$  cuts described there. The neutral current background ( $\nu_\mu N \rightarrow \nu_\mu X$ ) still remains, but the measured neutrino energy will be smaller than the predicted value because of the missing outgoing neutrino. The distribution of  $\Delta E_\nu/E_\nu$  (tagger-to-neutrino-detector) can then be used; we cut on missing energy of  $>25\%$  and lose  $1/3$  of the sample but eliminate this background.

Finally, we can think of no significant background in the cross-section determinations. The cross-section will be calculated by forming a ratio proportional to the cross-section:

$$R_\nu = \frac{\text{(observed } \nu \text{ with a tag)}}{\text{(random prescaled sample from the tagger)}}$$

The dominant systematic error will be the error in predicting whether the neutrino will strike the detector for events in the denominator. By cutting away from the edges of the neutrino detector, we can increase the acceptance to 90% and are confident the systematic error on the acceptance will be 1% or less. We expect the final cross-section sample to be 25K for  $\nu_e$  and 16K for  $\nu_\mu$ . In each,  $2/3$  will be neutrino and  $1/3$  antineutrino (from the relative neutrino/antineutrino cross-section) so the statistical errors will always be under 2%.

## VI. Schedule

We are currently negotiating with other experimental groups and expect that the requisite



manpower will exist by Spring, 1989. Construction could begin in 1990 with a first run in 1991 which will "shake-down" the detector and provide our first data sample. The following fixed target run would provide our main sample. The experiment would then complete data-taking in approximately 1994.

## VII. Long Term $K_L$ Studies

The beam as planned could provide more than  $10^{14}$   $K_L$  per year. This is four to five orders of magnitude more  $K_L$  than have been seen in the best rare  $K_L$  decay experiments at Brookhaven. Triggering in such an environment is extremely difficult; furthermore, the detector is probably not optimized for the delicate background rejection required. However, with a lower rate and a better-defined decay region, we could think about a rare  $K_L$  decay search at the  $10^{-13}$  level. We are discussing the long-term possibilities with the "Future of Kaon Physics" committee at Fermilab (B. Winstein, chair).

## VIII. Summary

We have demonstrated the physics potential of the tagged neutrino line to significantly extend the  $\nu_e \rightarrow \nu_\mu$  and  $\nu_\mu \rightarrow \bar{\nu}_\mu$  limits, probe an important region of mixing in  $\nu_e \rightarrow \nu_\tau$ , and perform precision measurements of the  $\nu_e$  and  $\nu_\mu$  cross-sections at the 1-2% level. The calculated fluxes are based on extensive experience at FNAL. The design of the tagging spectrometer, although obviously preliminary, is within standard practice. In two fixed target runs we can explore new neutrino oscillation physics and provide benchmark cross-section measurements that are perhaps uniquely accessible with tagged neutrinos.